Iranian Polymer Journal (2023) 32:1179–1188
https://doi.org/10.1007/s13726-023-01194-5

ORIGINAL RESEARCH

Poly(*L*-lactic acid)/poly(ethylene oxide) electrospun scaffold containing dexamethasone-loaded TiO_2–alendronate mesoporous nanoparticles utilized for bone tissue engineering application

Marziyeh Motiei Pour[1] · Mohammad Reza Moghbeli[1] · Bagher Larijani[2] · Hamid Akbari Javar[3]

Received: 19 October 2022 / Accepted: 15 May 2023 / Published online: 27 June 2023

Abstract

In this work, asymmetrically poly(*L*-lactic acid)/poly(ethylene oxide) (PLLA/PEO) electrospun scaffolds were incorporated with novel mesoporous TiO_2–alendronate nanoparticles loaded with dexamethasone (Dex–TiO_2–ALN). The impact of nanoparticle incorporation on the fibers morphology and mechanical properties of the scaffolds was evaluated using FESEM technique and tensile stress assessments, respectively. After the investigation of the release behavior of the scaffolds, in vitro cell studies were performed employing MTT assay for cell viability assessment. Additionally, alkaline phosphatase (ALP) activity and calcium deposition assays were carried out for the potential determination of the osteogenic differentiation of the fabricated scaffolds on human adipose tissue-derived mesenchymal stem cells (hA-MSCs). The results showed that the incorporation of the nanoparticles decreased the average diameter of the electrospun fibers from 693 nm for the neat PLLA/PEO scaffold to 640 nm and 643 nm for the scaffolds containing TiO_2–alendronate (TiO_2–ALN) and Dex–TiO_2–ALN nanoparticles, respectively. However, the surface morphology of the fibers did not changed significantly. According to the mechanical test results, the maximum strengths at breakpoint were 1.20, 1.27, and 1.28 MPa for the neat PLLA/PEO mat and its TiO_2–ALN and Dex–TiO_2–ALN-reinforced samples, respectively. The release profile showed an initial burst release around 11% of initial loaded Dex after 72 h, followed by a gradual increase to 38.23% at the end of the release period. Moreover, introducing Dex–TiO_2–ALN nanoparticles improved cell viability, ALP activity, and calcium deposition as well as notified the importance of scaffold engineering for biomedical applications.

✉ Mohammad Reza Moghbeli
mr_moghbeli@iust.ac.ir

[1] Smart Polymers and Nanocomposites Research Group, School of Chemical Engineering, Iran University of Science and Technology, Tehran 16846–13114, Iran

[2] Endocrinology and Metabolism Research Centre, Tehran University of Medical Sciences, Tehran, Iran

[3] Department of Pharmaceutics, Faculty of Pharmacy, Tehran University of Medical Sciences, Tehran, Iran

Graphical abstract

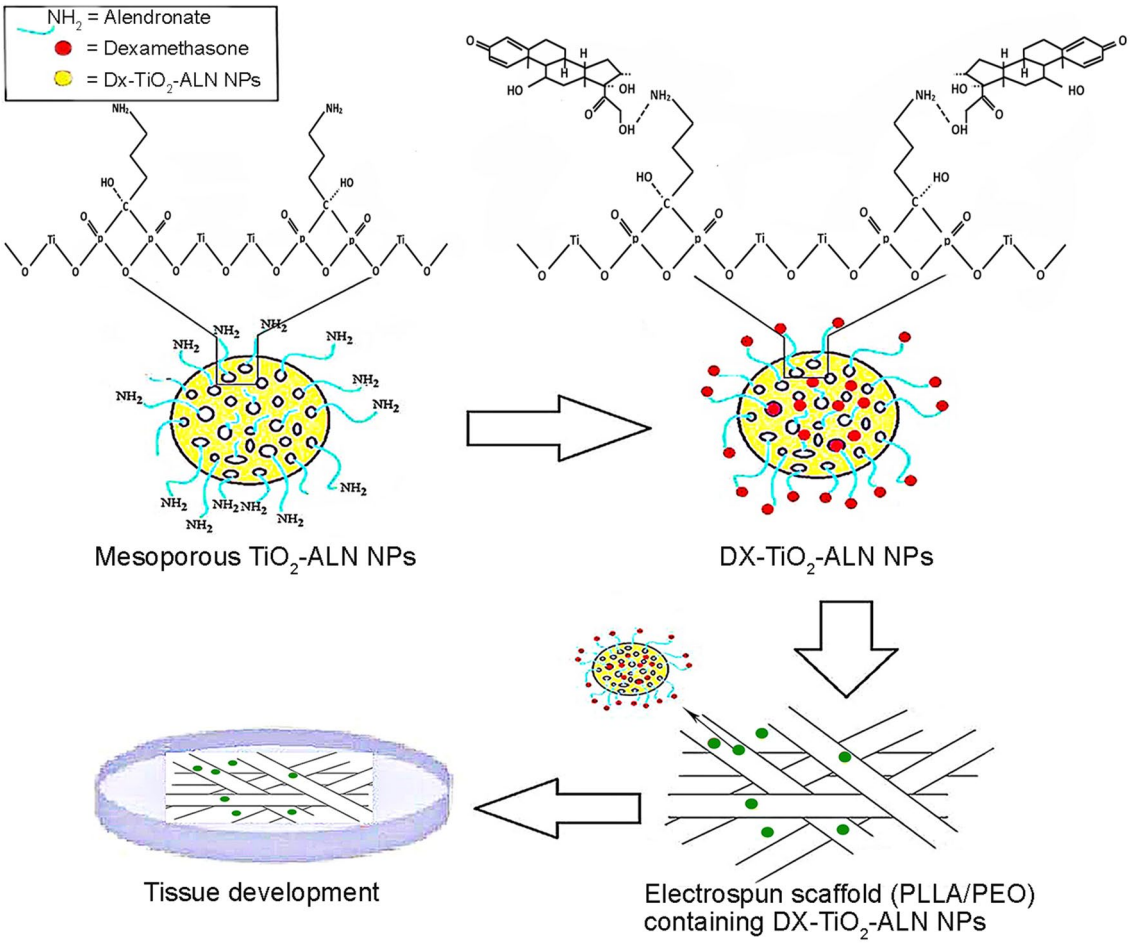

Keywords Bone tissue engineering · Electrospinning · Poly(*L*-lactic acid)/poly(ethylene oxide) electrospun scaffold · TiO_2–alendronate nanoparticles · Dexamethasone

Introduction

Tissue engineering is one of the best-known ways of dealing with tissue defects. The goal of tissue engineering is to regenerate new tissues for replacing the damaged ones [1]. A scaffold is an important part of the tissue engineering process which has several requirements [2]. An excellent scaffold for bone tissue engineering shall match various criteria involving open porosity, compressive intensity, and usefulness for cell migration [3].

Various preparation techniques, such as spray drying, phase separation, chemical vapor deposition, electrospinning, and nano-imprinting, have been used to fabricate fibrous scaffolds [4]. Electrospinning is an attractive method to prepare scaffolds for bone tissue [5]. Some biodegradable polymers, such as poly(*L*- lactic acid) (PLLA), poly(glycolic acid) (PGA), poly(lactic-*co*-glycolic acid) (PLGA), and polycaprolactone (PCL) are mainly used for scaffold manufacturing [6]. Poly(*L*-lactic acid) (PLLA) is one of the most widely used FDA-approved synthetic polymers for scaffold production [7]. Along with the desirable characteristics of PLLA, such as biocompatibility, biodegradability, and easy fabrication process, there are some disadvantages for pure PLLA scaffolds, including low mechanical strength, acidic byproduct production, and inflammation responses [8].

Some studies were carried out on modifying PLLA scaffolds to improve cell adhesion and migration, proliferation, and differentiation on the scaffold surface [7–9]. Composite making with polymeric or ceramic nanoparticles is another attractive approach. Due to the rapid development of the tissue engineering field, some PLLA modifiers were employed to address the challenges of using neat PLLA scaffolds, including low degradation rate and hydrophobicity [9, 10]. To prepare a PLLA-based scaffold

with a more desirable degradation rate and hydrophilic characteristics, poly(ethylene oxide) (PEO) is usually utilized as an excellent candidate to blend with PLLA [10, 11]. In addition, adding PEO would improve the biocompatibility and cost-effectivity of the resultant PLLA scaffolds. Therefore, adding PEO to PLLA improved the hydrophilicity, flexibility, and degradation period of the PLLA-based scaffolds [12, 13].

Recently, a wide variety of polymeric nanoparticles (NPs) [14–16], nanocomposites [17, 18], and nano-complexes [19, 20] have been fabricated to improve the performance of carriers. Incorporating inorganic porous nanoparticles into scaffolds improved the controlled drug delivery [7]. These nanocarriers provided a high specific surface area and improved drug release in a controlled manner. Qiu et al. [21] developed a poly(*L*-lactic acid)/poly(ε-caprolactone) nanofibrous scaffold containing dexamethasone (Dex)-loaded silica NPs for bone tissue engineering applications. While samples with NPs showed higher biocompatibility of cultured rat bone marrow-derived mesenchymal stem cells, higher amounts of osteogenic differentiation were also obtained during in vitro studies. The effectiveness of scaffolds incorporated with nanoparticles proved that the nanoparticles-loaded scaffolds remarkably promoted calvarial defect healing in Sprague-Dawley (SD) rats [22].

Titania (TiO_2) is a biomaterial that seems attractive because of its superior mechanical behavior and higher biocompatibility [23]. The mesoporous TiO_2 NPs provided numerous benefits over non-porous ones. The former decentralized stress provided needed space for new bone mass ingrowths, enhanced osseointegration, and provided great ability for apatite structure and protein absorption [24]. Specific properties of mesoporous titanium dioxide (TiO_2) NPs also make them a potential additive for preparing biomedical scaffolds. Ma et al. developed surface-functionalized metal oxides-based carriers with phosphonates to prepare hybrid phosphonate–TiO_2 mesoporous NPs [22].

Recently, alendronate (ALN), a third-generation bisphosphonate, has been used for bone targeting agents, bone differentiation conductors, and osteoclast apoptosis simulator [25–27]. Alendronate (ALN) was also used for surface functionalization of NPs. For instance, ALN was coated on silver NPs surfaces to make a pH-sensitive dual drug-delivery system [28]. Incorporating the pH-sensitive ALN agent into the structure of nanoparticles and exposing the resulting functionalized NPs to the acidic pH of endosomes after cell uptake, led to the effective release of encapsulated ingredients into the cytosol [7]. In addition, it was shown that the application of ALN decreased the cytotoxicity of the TiO_2 surface and improved bone growth in bone implants [29, 30]. Moreover, it was possible to improve drug contents within mesoporous NPs using the ALN molecules owing to their functional groups [31, 32].

Although silica nanoparticles (MSNs) have been mainly prepared for drug delivery purposes, less attention has been paid to preparing non-silica-based substitutes. Mesoporous titanium dioxide (TiO_2) NPs can be considered as promising metal-oxide carriers. These NPs would provide a high surface area with uniform pore size, biocompatibility, and low toxicity. These characteristics make them desirable for biomedical applications, including anticancer agents, and implants [33–35].

Despite some studies have been done on preparing drug-loaded SiO_2 NPs reinforced electrospun fibers, less attention has been paid to manufacturing electrospun fibers containing Dex–TiO_2–ALN NPs for drug delivery. For this purpose, pH-sensitive TiO_2–ALN NPs containing Dex (Dex–TiO_2–ALN) NPs were prepared by modified ionic liquid-assisted method. After that, the prepared NPs were incorporated into PLLA/PEO microfibers prepared via electrospinning, released drugs in a predetermined manner. Dexamethasone (Dex) would induce in vitro osteogenic differentiation of mesenchymal stem cells (MSCs) through attachment to glucocorticoid receptor of cellular cytosol. To assess the MSCs' osteogenic differentiation capability of the prepared scaffolds, alkaline phosphate activity (ALP) and calcium deposition were also measured.

Experimental

Materials

Dichloromethane, dimethylformamide, PLLA (average MW of 240,000 g/mol), and PEO (average MW of 900,000 g/mol) were purchased from Sigma-Aldrich and used without any further purification. Titanium tetrachloride ($TiCl_4$), alendronate sodium trihydrate (AST), the room-temperature ionic liquid 1-butyl-3-methyl-imidazolium-tetra fluoroborate (RTIL-1), cetyltrimethylammonium bromide (CTAB) were purchased from Sigma-Aldrich (St. Louis, MO), while dexamethasone (Dex), ethanol and acetonitrile were prepared from Merck (Darmstadt, Germany). Dulbecco's Modified Eagle's Medium (DMEM), RPMI1640 medium, fetal bovine serum (FBS), and trypsin–EDTA were prepared from Gibco/Life Technologies (USA). 3-(4,5-Dimethylthyazolyl-2)-2,5-diphenyl tetrazolium bromide (MTT, ICN Biomedicals Inc., USA) was used. ALP activity assay kit (Parsazmoon, Tehran, Iran) was purchased. Deionized distilled water (DDI) was prepared in the authors' lab.

Methods

Preparation of TiO_2–ALN NPs

The synthesis method of spherical mesoporous phosphonate–TiO_2 was described more in detail elsewhere [31]. The

synthesis process was carried out using a modified ionic liquid-assisted form. An aqueous solution of CTAB was prepared by adding 0.6 g of CTAB to 2 mL of DDI under a vigorous stirring condition at room temperature. Then, 1 mL of titanium tetrachloride ($TiCl_4$) and 10 mL of (RTIL-1) were added to the prepared solution, and the mixture was heated at 80 °C for 2 h. An ALN sodium trihydrate solution was added to the reacting mixture (Ti/P = 3.6 molar ratio) at 80 °C for 12 h. Finally, further washing and purification stages were carried out. After that, Dex was loaded into the TiO_2–ALN NPs based on the following procedure. Amount of 0.2 mg of the TiO_2–ALN NPs was added into 20 mL Dex solution with concentration of 10 mg/mL and stirred at room temperature for 48 h [32].

Preparation of electrospinning solution

Amount of 0.43 g of PLLA (7%w/v) was dissolved in 6 mL of chloroform under stirring condition. The optimized amount of DMF (1 mL) was added to the mixture to obtain a transparent solution. PCL/PEO solutions were then prepared at different weight ratios, i.e., 95:5, 90:10, and 85:15 under stirring overnight at room temperature to obtain a homogenous solution [36, 37]. Amounts of 5%w/v of the prepared pristine TiO_2–ALN NPs (unloaded) and Dex-loaded TiO_2–ALN (Dex–TiO_2–ALN) NPs were added separately to the electrospinning solution for the preparation of nanocomposite scaffolds [7].

Scaffolds fabrication by electrospinning method

Scaffolds were prepared by electrospinning technique with an average thickness close to 0.2 mm. A syringe pump was used to inject the solutions through a stainless steel 18G needle (KDS 100, KD Scientific, Holliston, MA, USA). The flow rate was set for all specimens at 0.5 mL/h. The polymer fibers were collected on an aluminum foil wrapped on a drum by applying high voltages (10–18 kV) on the needle. All the electrospinning experiments were performed by electrospinning instrument (Electroris®) (Fanavaran Nano-Meghyas Co., Iran) at room temperature [38].

Scaffolds characterization

Morphology assessment

Morphology of the electrospun mats was evaluated by a field emission scanning electron microscope (FESEM, FEI Nova NanoSEM 450, USA). All samples were fixed on the aluminum grids, and a thin layer (10 nm) of gold was sputtered on the surface of the piece. ImageJ software was used for image processing of FESEM micrographs.

Inductively coupled plasma mass spectrometry (ICP-MS) as an analytical technique, was used to detect a broad range of species (1 ppt to 1 ppb) in the samples. To examine the presence of the nanoparticles within the fibers, the concentration of phosphorous ions obtained from the scaffolds was analyzed by ICP-MS. After digestion of samples in nitric acid for getting a homogenous solution, the solutions were introduced to a plasma stream leading to atomization and, subsequently, ionization of the material. Afterward, a conventional mass spectrometer measured the concentration of each species simultaneously [39].

Mechanical properties assessment

The dimensions of the fabricated scaffolds were precisely adjusted into a rectangular shape (30 mm × 5 mm × 70 µm). The crosshead speed and load cell capacity of the testing machine (SANTAM STM-20, Iran) were set at 5 mm/min and 5N, respectively [7]. Each experiment was repeated three times, and an average value was reported for each sample.

In vitro dexamethasone release

To investigate the cumulative release behavior of Dex from PLLA scaffolds containing Dex–TiO_2–ALN NPs, rectangular mats were immersed in 3 mL of PBS solution and incubated at 37 ºC under stirring condition for 21 days. At predetermined timepoints, the amount of released Dex was determined by UV–Visible (UV) spectrophotometer (Thermo Scientific NanoDrop™ 2000/2000c, USA) at 242 nm. Pure PLLA nanofibrous scaffolds were considered as blanks.

In vitro cell studies

Cell viability assessment

Before exposing scaffolds to viability evaluations, they were sterilized using ethanol (70%v/v) and washed with PBS. Then, 5×10^3 hA-MSCs (Passage 3, Royan Institute, Tehran, Iran) were cultured on scaffolds with standard cell culture media containing 10 (%v/v) FBS/DMEM. After 1, 3, and 5 days of cell seeding, the culture media was substituted by MTT solution (10%v/v) and incubated for 4 h. The ELISA reader (BioTech, USA) was used to determine the formed formazan crystals' absorbance at 570 nm [8]. The results were determined as means ± SD (n > 3).

Osteogenic differentiation assays

ALP activity assay kit was used to evaluate osteogenic differentiation of cells cultured on the scaffolds at days 7, 14,

and 21, according to its producer's guidance. Briefly, the determined volume of radioimmunoprecipitation assay (RIPA) buffer was added to the samples and then shaken for 1 h at 4 °C. The final solutions were centrifuged for 15 min at 15,000 rpm before adding *p*-nitrophenyl phosphate. An ELISA reader (BioTech, USA) detected the yellow color product at 405 nm [9].

According to the producer's guidance, the deposited calcium was evaluated by a calcium assay kit (Parsazmoon, Tehran, Iran) on days 7, 14, and 21. Briefly, the deposited calcium interacted with Arsenozo III, and the colored products were collected and read by an ELIZA reader at 630 nm [9].

Statistical analysis

All experiments were repeated at least three times, and the results were reported as the mean ± SD. The two-way ANOVA was performed to analyze the significant differences by employing GraphPad Prism 8. Through this work, the p-values were considered as $*p < 0.05$, $**p < 0.01$, $***p < 0.001$, and $****p < 0.0001$.

Results and discussion

This study mainly focuses on preparing PLLA/PEO fibrous scaffolds containing novel Dex–TiO_2–ALN NPs and delivering Dex to enhance osteogenic differentiation of hA-MSCs. The fabricated scaffolds were evaluated to investigate how much they could facilitate the osteogenic differentiation of MSCs.

Morphology and content evaluation of the scaffolds

Figure 1 indicates the morphology of the neat PLLA/PEO scaffold and scaffolds containing 5 wt% of TiO_2–ALN and Dex–TiO_2–ALN NPs. The PLLA/PEO blend ratio of 90/10 (wt%/wt%) was used for all the scaffolds. As shown by FESEM micrographs, all the samples were bead-free with a smooth surface. The incorporation of the nanoparticles did not significantly change the surface morphology of the electrospun fibers. However, the nanoparticles are observed on the nanocomposite fibers. The fiber diameter of the prepared scaffolds was analyzed by ImageJ software. Figure 2 indicates the distribution of microfiber diameters of the neat and nanocomposite scaffolds. As can be seen, an average diameter of 693, 640, and 643 nm was obtained for the neat PLLA/PEO scaffold, TiO_2–ALN NPs, and Dex–TiO_2–ALN nanoparticles PLLA/PEO reinforced scaffolds, respectively. The observed changes in the fiber diameter can be attributed to solution viscosity change and electric conductivity reduction after adding the nanoparticles [40]. The final viscosity of the electrospinning solution plays a crucial role in determining fiber diameters. Cho et al. [10] studied the effect of solution viscosity on the fabricated PCL scaffold properties. According to the ICP-MS assay, the TiO_2–ALN NPs scaffolds contain 0.018% Ti and 0.003% P.

Tensile strength

The tensile strength of a nanofibrous scaffold has a determining impact on cellular fates employed in bone tissue engineering [26]. To put it differently, it is essential to evaluate the tensile properties of the fabricated scaffolds before using them for bone tissue engineering purposes. Characteristics such as stress, strain, and elastic modulus should be precisely tuned to maximize the osteogenic differentiation ability of MSCs [33].

To assess the effect of added nanoparticles on the mechanical characteristics of the prepared scaffolds, the stress–strain behavior of the neat and reinforced PLLA/PEO scaffolds is evaluated in Fig. 3. As shown in the figure, the maximum strengths at the breakpoints are 1.20, 1.27, and 1.28 MPa for the neat PLLA/PEO, and its mats with nanoparticles of TiO_2–ALN and Dex–TiO_2–ALN, respectively. Also, the measured elongations-at-break point were 103.55, 99.71, and 100.57 for the neat, TiO_2–ALN- and Dex–TiO_2–ALN-reinforced PLLA/PEO mats, respectively. Moreover, although the Young's modulus was 2.53 MPa for the PLLA/PEO mat, it was decreased to a fixed amount of 1.89 MPa for the reinforced mats. Therefore, the addition of 5 wt% nanoparticles into the PLLA/PEO scaffolds has no significant effect on their mechanical strength [8]. Porgham-Daryasari et al. [7] showed that incorporation of mesoporous silica nanoparticles within PLLA nanofibrous scaffolds enhanced the mechanical strength of the reinforced PLLA scaffolds, significantly.

In vitro dexamethasone release profile

To investigate osteogenic differentiation in three weeks, the release profile of scaffolds containing Dex was examined within 21 days. Figure 4 indicates an initial burst release close to 11% after 72-h elapsed time of releasing process. The release was gradually increased to 38.23% at the end of the release period. The release profile was similar to the release profiles obtained for PLLA-(PLLA-Dexa-P123)-PLLA-P123 sample [4].

In vitro studies

Cell attachment and proliferation

To determine the proper amount of PEO in the PLLA/PEO-fabricated scaffold, electrospinning solutions based

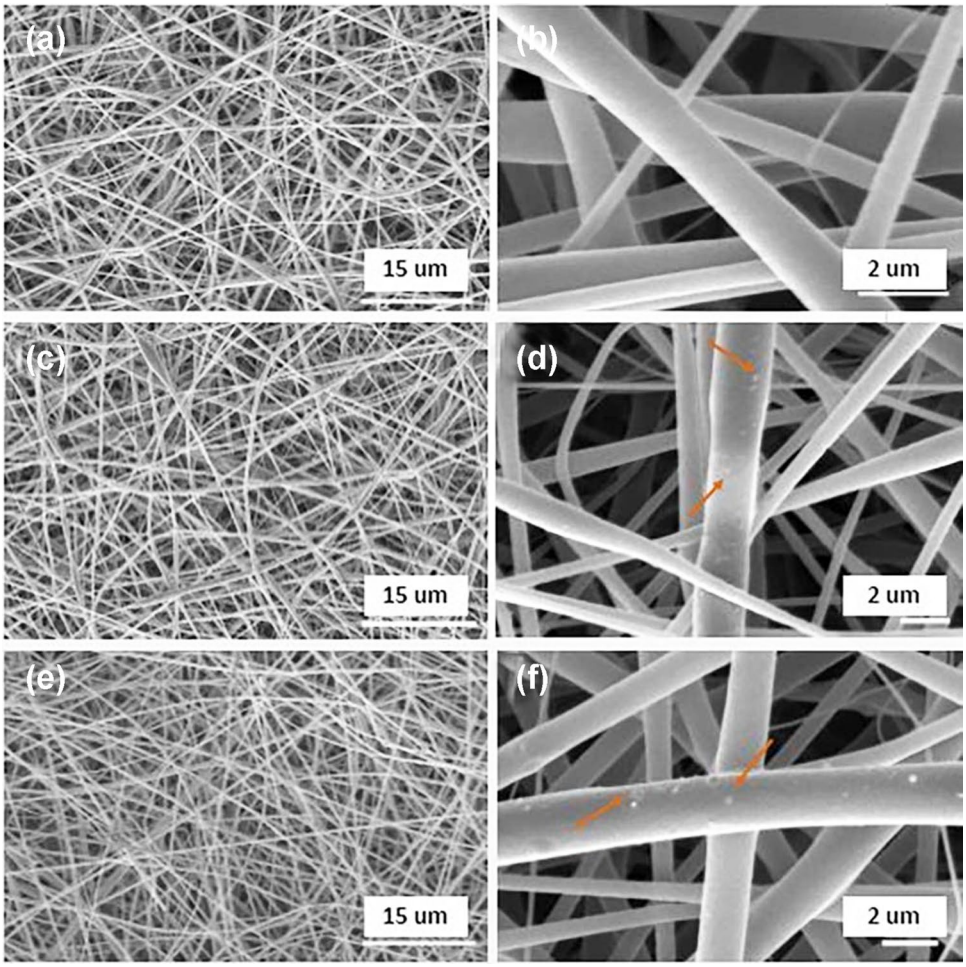

Fig. 1 FESEM micrographs of the electrospun nanofibrous scaffolds: **a**, **b** pure PLLA/PEO 10%, **c**, **d** PLLA/PEO10%/TiO_2–ALN NPs, and **e**, **f** PLLA/PEO10%/Dex–TiO_2–ALN NPs (Arrows indicate the incorporated nanoparticles on the fibers surface)

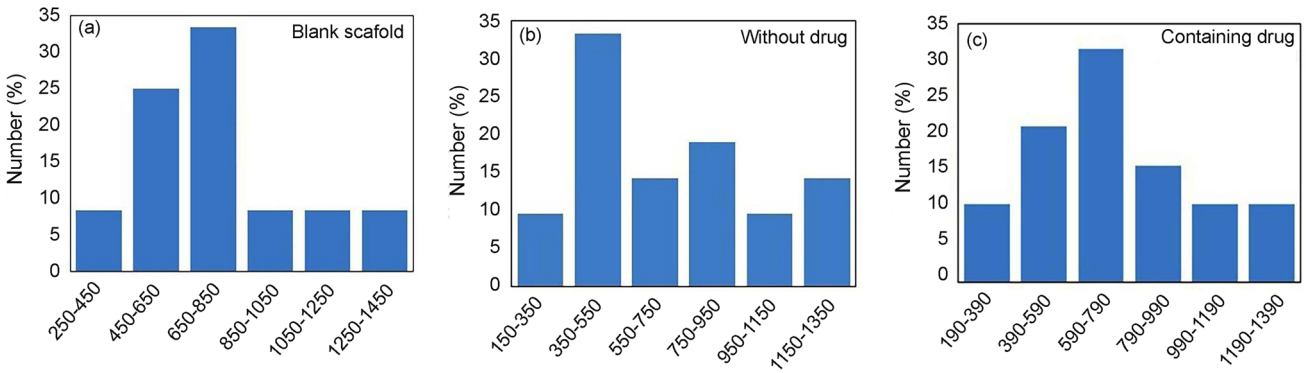

Fig. 2 Fiber diameter distributions of: **a** pure PLLA/PEO10%, **b** PLLA/PEO10%/TiO_2–ALN NPs, and **c** PLLA/PEO10%/Dex–TiO_2–ALN NPs

on three different PEO weight percentages, i.e., 5, 10, and 15 were prepared. However, the PLLA scaffold was also fabricated for comparison purposes. Then, cell proliferation characteristics of the cells cultured on the resultant scaffolds were assumed as the criterion of excellence. The MTT assay was performed after 1, 3, and 5 days.

As shown in Fig. 5, there is no significant difference in cell viability between the neat PLLA and PLLA/PEO scaffolds on first day. The incorporation of 10 and 5 wt% PEO to the PLLA improved the cell viability of the fabricated scaffold after 3 and 5 days (***P > 0.001, ****P > 0.0001).

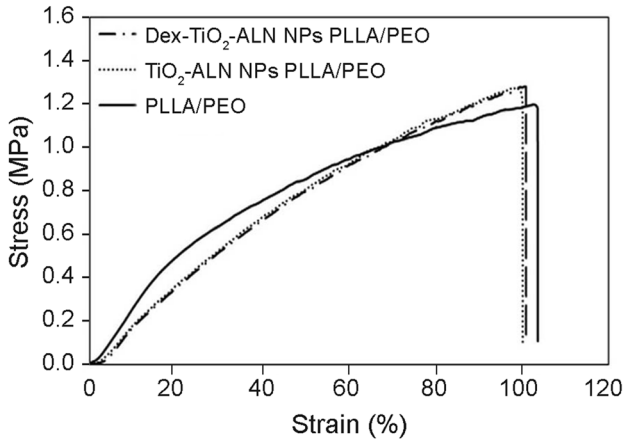

Fig. 3 Stress–strain curves of the PLLA/PEO10%, PLLA/PEO10%/TiO_2–ALN NPs, and PLLA/PEO10%/Dex–TiO_2–ALN NPs mats. (Maximum forces at breakpoints: 1.2, 1.26, and 1.28 MPa for the neat PLLA/PEO10%, PLLA/PEO10%/TiO_2–ALN NPs, and PLLA/PEO10%/Dex–TiO_2_ALN NPs, respectively)

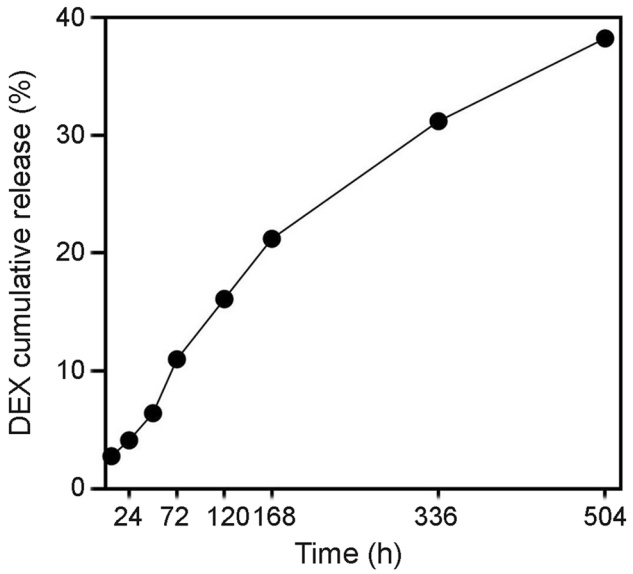

Fig. 4 Dexamethasone release behavior assessment of PLLA/PEO10%/Dex–TiO_2–ALN NPs

Overall, the highest cell viability was observed in the order of PLLA/PEO10% > PLLA/PEO5%.

For the scaffold with the highest PEO content (PLLA/PEO15%), the least cell viability was obtained after days 3 and 5 (Fig. 5). This behavior can be connected to the higher scaffold degradation in compression with other scaffolds with lower PEO contents. Higher PEO content resulted in hydrophilicity enhancement and cell detachment [10]. Therefore, the PLLA/PEO10% was selected as the best candidate to prepare nanocomposite scaffolds.

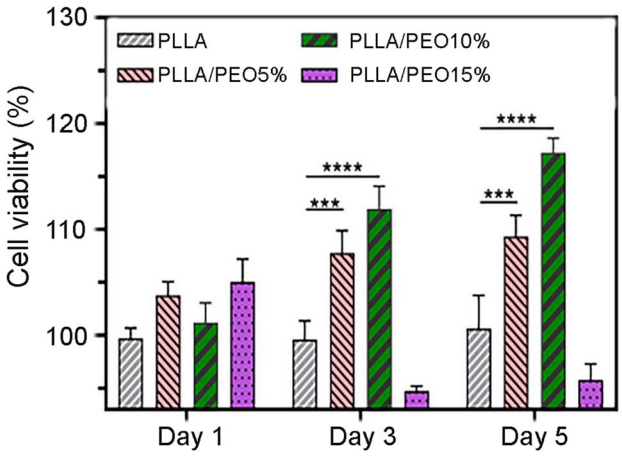

Fig. 5 Optimizing of the PEO compartment into the scaffolds by MTT assessment (PLLA/PEO10% showed the highest cell viability compared to other specimens with higher and lower PEO content (***$P < 0.001$ and ****$P < 0.0001$))

The proliferation of the cells cultured on the neat and nanocomposite scaffolds without and with Dex was assessed by MTT assays on days 1, 3, and 5 (Fig. 6a). The engineered scaffolds could improve the viability of the cells slightly. There were no significant viability differences between the drug-unloaded and drug-loaded PLLA/PEO10% scaffolds. However, all groups had significant differences in tissue culture plate (TCP). This improvement was mainly due to changes in fibers diameter. The fibers with smaller diameters exhibit a higher surface-to-volume ratio [7]. To put it differently, an increase in this ratio leads to having a more accessible surface area for the cells' attachment to the surface. The same trend was repeated every three days. PLLA nanofibrous scaffolds have been one of the most desirable scaffolds for bone tissue engineering applications [32–34]. Porgham-Daryasari et al. [7] fabricated PLLA nanofibrous scaffolds containing Dex-loaded mesoporous silica nanoparticles showing the highest MSC cytocompatibility.

Osteogenic differentiation

The osteogenic differentiation possibility of human adipose mesenchymal stem cells (hA-MSCs) has been repeatedly investigated in a wide variety of studies [14, 41]. Many reasons can be accounted for employing hA-MSCs as a desirable candidate cell to assess osteogenic differentiation. There are significant osteogenic differentiation capabilities and fast cell proliferation compared to other MSCs [42]. Another equally essential advantages of hA-MSCs are their easy harvesting. Simply put, they can be extracted from a donor with the least invasion [43]. According to previous studies, the first stage for evaluating potential osteogenic differentiation is

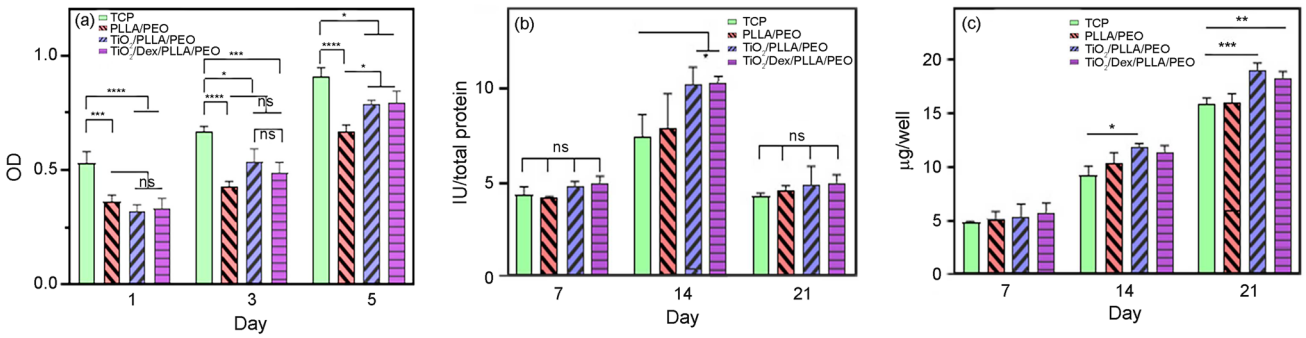

Fig. 6 In vitro cell studies: **a** evaluation of in vitro cell cytotoxicity by MTT assay at 1, 3, and 5 days after cell seeding, **b** effect of incorporating NPs into PLLA/PEO10% scaffolds on ALP activity of hA-MSCs, and **c** level of calcium depositions in the NPs-loaded groups at different time intervals (*$P<0.05$, **$P<0.01$, ***$P<0.001$ and ****$P<0.0001$)

assessing immature bone markers, which can be analyzed by ALP activity assessment. The late cues of osteogenic differentiation can be ECM secretion of calcium. Therefore, calcium deposition evaluation indicates successful osteoblast making, which can be examined by ALP activity assessment [44].

The ability of the fabricated scaffolds, i.e., the pure PLLA/PEO and its PLLA/PEO nanocomposites, to conduct osteogenic differentiation of MSC was evaluated by employing ALP activity and calcium deposition assays. Figure 6b shows the ALP activity analysis of hA-MSCs cultured on the mentioned scaffolds for 7, 14, and 21 days. There are no remarkable differences among the nanocomposite scaffolds and control group on day 7. As represented, the ALP activity of all the samples was raised from day 7 to day 14. On day 14, the nanocomposite scaffolds showed a significant ALP activity compared to the neat PLLA/PEO scaffold and the tissue culture plate (TCP). Calcium secretion amount would be an indicator of mature osteoblasts [8].

As shown in Fig. 6c, a remarkable increase was displayed through three time points. The highest calcium deposition was obtained after 21 days. In the bone regeneration process, polymeric nanofibers scaffolds needed to be improved to favor biological responses alongside assuming structural support. The addition of the prepared nanoparticles significantly enhanced the physicochemical properties of the PLLA/PEO scaffolds through successful delivery of the Dex-loaded nanoparticles for bone tissue engineering purposes. This was mainly possible because of the presence of the fabricated pH-sensitive nanoparticles that showed an accelerated drug release in an acidic pH environment like endosomal moieties [7]. The prepared nanocomposite scaffolds can be applied to conduct stem cell behavior toward bone.

Conclusion

In this study, the PLLA/PEO blend was engineered to prepare an electrospun nanocomposite scaffold by incorporating the novel Dex-TiO_2–ALN NPs for bone tissue engineering applications. The prepared scaffolds showed a desirable fibrous morphology and proper mechanical properties improving human adipose tissue-derived mesenchymal stem cells osteogenic differentiation in comparison with the neat PLLA nanofibrous scaffolds as the control group. According to the obtained desirable cell viability, ALP activity and calcium deposition was properly obtained for the PLLA/PEO10% scaffold containing Dex–TiO_2–ALN NPs. Therefore, this sample code was selected as the best group with the highest osteogenic differentiation potential. To verify the proper host–biomaterial interaction of this group, performing in vivo studies is suggested for future work.

Acknowledgements The authors appreciate the partial support from the Iran University of Science & Technology (IUST) and Tehran University of Medical Science.

Data availability Not available.

References

1. Kong B, Sun W, Chen G, Tang C, Li M, Shao Z, Mi S (2017) Tissue-engineered cornea constructed with compressed collagen and laser-perforated electrospun mat. Sci Rep 7:970. https://doi.org/10.1038/s41598-017-01072-0
2. Hosseinzadeh S, Zarei-Behjani Z, Bohlouli M, Khojasteh A, Ghasemi N, Salehi-Nik N (2022) Fabrication and optimization of bioactive cylindrical scaffold prepared by electrospinning for vascular tissue engineering. Iran Polym J 31:127–141
3. Liverani L, Raffel N, Fattahi A, Preis A, Hoffmann I, Boccaccini AR, Beckmann MW, Dittrich R (2019) Electrospun patterned

porous scaffolds for the support of ovarian follicles growth: a feasibility study. Sci Rep 9:1150. https://doi.org/10.1038/s41598-018-37640-1
4. Birhanu G, Tanha S, Akbari Javar H, Seyedjafar E, Zandi-Karimi A, Kiani-Dehkordi B (2019) Dexamethasone loaded multi-layer poly-l-lactic acid/pluronic P123 composite electrospun nanofiber scaffolds for bone tissue engineering and drug delivery. Pharm Dev Technol 24:338–347. https://doi.org/10.1080/10837450.2018.1481429
5. Atila D, Hasirci V, Tezcaner A (2022) Coaxial electrospinning of composite mats comprised of core/shell poly (methyl methacrylate)/silk fibroin fibers for tissue engineering applications. J Mech Behav Biomed Mater 128:105105. https://doi.org/10.1016/j.jmbbm.2022.105105
6. Maleki H, Semnani Rahbar R, Nazir A (2020) Improvement of physical and mechanical properties of electrospun poly (lactic acid) nanofibrous structures. Iran Polym J 29:841–851. https://doi.org/10.1007/s13726-020-00844-2
7. Porgham-Daryasari M, Dusti Telgerd M, Karami MH, Zandi-Karimi A, Akbarijavar H, Khoobi M, Seyedjafari E, Birhanu G, Khosravian P, Sadat-Mahdavi F (2019) Poly-l-lactic acid scaffold incorporated chitosan-coated mesoporous silica nanoparticles as pH-sensitive composite for enhanced osteogenic differentiation of human adipose tissue stem cells by dexamethasone delivery. Artif Cells Nanomed Biotechnol 47:4020–4029. https://doi.org/10.1080/21691401.2019.1658594
8. Telgerd MD, Sadeghinia M, Birhanu G, Porgham-Daryasari M, Zandi-Karimi A, Sadeghinia A, Akbarijavar H, Karami MH, Seyedjafari E (2019) Enhanced osteogenic differentiation of mesenchymal stem cells on metal–organic framework based on copper, zinc, and imidazole coated poly-l-lactic acid nanofiber scaffolds. J Biomed Mater Res Part A 107:1841–1848. https://doi.org/10.1002/jbm.a.36707
9. Zhu X, Zhong T, Huang R, Wan A (2015) Preparation of hydrophilic poly (lactic acid) tissue engineering scaffold via (PLA)-(PLA-b-PEG)-(PEG) solution casting and thermal-induced surface structural transformation. J Biomater Sci Polym Ed 26:1286–1296. https://doi.org/10.1080/09205063.2015.1088125
10. Ju J, Peng X, Huang K, Li L, Liu X, Chitrakar Ch, Chang L, Gu Z, Kuang T (2019) High-performance porous PLLA-based scaffolds for bone tissue engineering: Preparation, characterization, and in vitro and in vivo evaluation. Polymer (Guildf) 180:121707. https://doi.org/10.1016/j.polymer.2019.121707
11. Wang H, Di J, Sun Y, Fu J, Wei Z, Matsui H, del C Alonso A, Zhou S, (2015) Biocompatible PEG-chitosan@ carbon dots hybrid nanogels for two-photon fluorescence imaging, near-infrared light/pH dual-responsive drug carrier, and synergistic therapy. Adv Funct Mater 25:5537–5547. https://doi.org/10.1002/adfm.201501524
12. Zhang C, Wang L, Zhai T, Wang X, Dan Y, Turng L-S (2016) The surface grafting of graphene oxide with poly (ethylene glycol) as a reinforcement for poly (lactic acid) nanocomposite scaffolds for potential tissue engineering applications. J Mech Behav Biomed Mater 53:403–413. https://doi.org/10.1016/j.jmbbm.2015.08.043
13. Xie H, He M, Deng X-Y, Du L, Fan C-J, Yang K-K, Wang Y-Z (2016) Design of poly (L-lactide)–poly (ethylene glycol) copolymer with light-induced shape-memory effect triggered by pendant anthracene groups. ACS Appl Mater Interfaces 8:9431–9439. https://doi.org/10.1021/acsami.6b00704
14. Moradikhah F, Doosti-Telgerd M, Shabani I, Soheili S, Dolatyar B, Seyedjafari E (2020) Microfluidic fabrication of alendronate-loaded chitosan nanoparticles for enhanced osteogenic differentiation of stem cells. Life Sci 254:117768. https://doi.org/10.1016/j.lfs.2020.117768
15. Soheili S, Mandegar E, Moradikhah F, Doosti-Telgerd M, Akbari-Javar H (2021) Experimental and numerical studies on microfluidic preparation and engineering of chitosan nanoparticles. J Drug Deliv Sci Technol 61:102268. https://doi.org/10.1016/j.jddst.2020.102268
16. Farahani M, Moradikhah F, Shabani I, Soflou RK, Seyedjafari E (2021) Microfluidic fabrication of berberine-loaded nanoparticles for cancer treatment applications. J Drug Deliv Sci Technol 61:102134. https://doi.org/10.1016/j.jddst.2020.102134
17. Heydariyan Z, Monsef R, Salavati-Niasari M (2022) Insights into impacts of Co_3O_4-CeO_2 nanocomposites on the electrochemical hydrogen storage performance of g-C_3N_4: Pechini preparation, structural design and comparative study. J Alloys Compd 924:166564. https://doi.org/10.1016/j.jallcom.2022.166564
18. Monsef R, Salavati-Niasari M (2023) Architecturally robust tubular nano-clay grafted $Li_{0.9}Ni_{0.5}Co_{0.5}O_{2-x}$/LiFeO2 nanocomposites: new implications for electrochemical hydrogen storage. Fuel 332:126015. https://doi.org/10.1016/j.fuel.2022.126015
19. Salavati-Niasari M, Banitaba SH (2003) Alumina-supported Mn(II), Co(II), Ni(II) and Cu(II) bis(2-hydroxyanil)acetylacetone complexes as catalysts for the oxidation of cyclohexene with *tert*-butylhydroperoxide. J Mol Catal A Chem 201:43–54. https://doi.org/10.1016/S1381-1169(03)00128-6
20. Salavati-Niasari M, Farzaneh F, Ghandi M (2002) Oxidation of cyclohexene with *tert*-butylhydroperoxide and hydrogen peroxide catalyzed by alumina-supported manganese(II) complexes. J Mol Catal A Chem 186:101–107. https://doi.org/10.1016/S1381-1169(02)00045-6
21. Qiu K, Chen B, Nie W, Zhou X, Feng W, Wang W, Chen L, Mo X, Wei Y, He Ch (2016) Electrophoretic deposition of dexamethasone-loaded mesoporous silica nanoparticles onto poly(L-lactic acid)/poly(ε-caprolactone) composite scaffold for bone tissue engineering. ACS Appl Mater Interfaces 8:4137–4148. https://doi.org/10.1021/acsami.5b11879
22. Ma T-Y, Yuan Z-Y (2011) Metal phosphonate hybrid mesostructures: environmentally friendly multifunctional materials for clean energy and other applications. Chemsuschem 4:1407–1419. https://doi.org/10.1002/cssc.201100050
23. Liu S, Wu B, Yu Y, Shen Z (2019) Memory effect of arsenic-induced cellular response and its influences on toxicity of titanium dioxide nanoparticle. Sci Rep 9:107. https://doi.org/10.1038/s41598-018-36455-4
24. Crossland EJW, Noel N, Sivaram V, Leijtens T, Alexander-Webber JA, Snaith HJ (2013) Mesoporous TiO_2 single crystals delivering enhanced mobility and optoelectronic device performance. Nature 495:215–219. https://doi.org/10.1038/nature11936
25. Reszka AA, Rodan GA (2003) Mechanism of action of bisphosphonates. Curr Osteoporos Rep 1:45–52. https://doi.org/10.1007/s11914-003-0008-5
26. Bai S-B, Liu D-Z, Cheng Y, Cui H, Liu M, Cui M-X, Mei Q-B, Zhou S-Y (2019) Osteoclasts and tumor cells dual targeting nanoparticle to treat bone metastases of lung cancer. Nanomedicine 21:102054. https://doi.org/10.1016/j.nano.2019.102054
27. Hochdörffer K, Abu Ajaj K, Schäfer-Obodozie C, Kratz F (2012) Development of novel bisphosphonate prodrugs of doxorubicin for targeting bone metastases that are cleaved pH dependently or by cathepsin B: synthesis, cleavage properties, and binding properties to hydroxyapatite as well as bone matrix. J Med Chem 55:7502–7515. https://doi.org/10.1021/jm300493m
28. Benyettou F, Rezgui R, Ravaux F, Jaber T, Blumer K, Jouiad M, Motte L, Olsen JC, Platas-Iglesias C, Magzoub M, Trabolsi A (2015) Synthesis of silver nanoparticles for the dual delivery of doxorubicin and alendronate to cancer cells. J Mater Chem B 3:7237–7245. https://doi.org/10.1039/x0xx00000x
29. Harmankaya N, Karlsson J, Palmquist A, Halvarsson M, Igawa K, Andersson M, Tengvall P (2013) Raloxifene and alendronate containing thin mesoporous titanium oxide films improve implant

fixation to bone. Acta Biomater 9:7064–7073. https://doi.org/10.1016/j.actbio.2013.02.040
30. Jeon C, Oh KC, Park K-H, Moon HS (2019) Effects of ultraviolet treatment and alendronate immersion on osteoblast-like cells and human gingival fibroblasts cultured on titanium surfaces. Sci Rep 9:2581. https://doi.org/10.1038/s41598-019-39355-3
31. Motiei Pour M, Moghbeli MR, Larijani B, Akbari Javar H (2022) pH-Sensitive mesoporous bisphosphonate-based TiO_2 nanoparticles utilized for controlled drug delivery of dexamethasone. Chem Pap 76:439–451. https://doi.org/10.1007/s11696-021-01870-x
32. Li H, Ma T-Y, Kong D-M, Yuan Z-Y (2013) Mesoporous phosphonate–TiO_2 nanoparticles for simultaneous bioresponsive sensing and controlled drug release. Analyst 138:1084–1090. https://doi.org/10.1039/c2an36631b
33. Carbone R, Marangi I, Zanardi A, Giorgetti L, Chierici E, Berlanda G, Podestà A, Fiorentini F, Bongiorno G, Piseri P, Pelicci PG, Milani P (2006) Biocompatibility of cluster-assembled nanostructured TiO_2 with primary and cancer cells. Biomaterials 27:3221–3229. https://doi.org/10.1016/j.biomaterials.2006.01.056
34. Kar A, Raja KS, Misra M (2006) Electrodeposition of hydroxyapatite onto nanotubular TiO_2 for implant applications. Surf Coatings Technol 201:3723–3731. https://doi.org/10.1016/j.surfcoat.2006.09.008
35. Cooper LF, Zhou Y, Takebe J, Guo J, Abron A, Holmén A, Ellingsen JE (2006) Fluoride modification effects on osteoblast behavior and bone formation at TiO_2 grit-blasted cp titanium endosseous implants. Biomaterials 27:926–936. https://doi.org/10.1016/j.biomaterials.2005.07.009
36. Seyedjafari E, Soleimani M, Ghaemi N, Shabani I (2010) Nanohydroxyapatite-coated electrospun poly(l-lactide) nanofibers enhance osteogenic differentiation of stem cells and induce ectopic bone formation. Biomacromolecules 11:3118–3125. https://doi.org/10.1021/bm1009238
37. Karimi Z, Seyedjafari E, Mahdavi FS, Hashemi SM, Khojasteh A, Kazemi B, Mohammadi-Yeganeh S (2019) Baghdadite nanoparticle-coated poly l-lactic acid (PLLA) ceramics scaffold improved osteogenic differentiation of adipose tissue-derived mesenchymal stem cells. J Biomed Mater Res A 107:1284–1293. https://doi.org/10.1002/jbm.a.36638
38. Ahmadi M, Seyedjafari E, Zargar SJ, Birhanu G, Zandi-Karimi A, Beiki B, Tuzlakoglu K (2017) Osteogenic differentiation of mesenchymal stem cells cultured on PLLA scaffold coated with Wharton's Jelly. EXCLI J 16:785–794. https://doi.org/10.17179/excli2016-741
39. Kwon KC, Jo E, Kwon Y-W, Lee B, Ryu JH, Lee EJ, Kim K, Lee J (2017) Superparamagnetic gold nanoparticles synthesized on protein particle scaffolds for cancer theragnosis. Adv Mater 29:1701146. https://doi.org/10.1002/adma.201701146
40. Rungswang W, Kotaki M, Shimojima T, Kimura G, Sakurai S, Chirachanchai S (2014) Role of surfactant on inducing specific microdomains of block copolymer: an example case from polystyrene-b-poly(ethylene-*co*-1-butene)-b-polystyrene (SEBS) electrospun thermoplastic-elastomer fiber containing polyethylene glycol lauryl ether (PGLE). Polymer (Guildf) 55:2068–2076. https://doi.org/10.1016/j.polymer.2014.02.057
41. Alonso-Goulart V, Ferreira LB, Duarte CA, Lima IL, Ferreira ER, Oliveira BC, Vargas LN, Moraes DD, Silva IBB, de Oliveira FR, Souza AG, de Souza C-F (2018) Mesenchymal stem cells from human adipose tissue and bone repair: a literature review. Biotechnol Res Innov 2:74–80. https://doi.org/10.1016/j.biori.2017.10.005
42. Burrow KL, Hoyland JA, Richardson SM (2017) Human adipose-derived stem cells exhibit enhanced proliferative capacity and retain multipotency longer than donor-matched bone marrow mesenchymal stem cells during expansion in vitro. Stem Cells Int 2017:2541275. https://doi.org/10.1155/2017/2541275
43. Yarak S, Okamoto OK (2010) Human adipose-derived stem cells: current challenges and clinical perspectives. An Bras Dermatol 85:647–656. https://doi.org/10.1590/S0365-05962010000500008
44. Yun Y-P, Kim S-J, Lim Y-M, Park K, Kim H-J, Jeong S-I, Kim SE, Song H-R (2014) The effect of alendronate-loaded polycarprolactone nanofibrous scaffolds on osteogenic differentiation of adipose-derived stem cells in bone tissue regeneration. J Biomed Nanotechnol 10:1080–1090. https://doi.org/10.1166/jbn.2014.1819